JOURNAL OF PROPULSION AND POWER
Vol. 24, No. 5, September–October 2008

Molecular Dynamics Simulation of Ion Emission from Nanodroplets of Ionic Liquids

John W. Daily*
University of Colorado at Boulder, Boulder, Colorado 80309-0427

DOI: 10.2514/1.28762

The work reported here is motivated by a desire to fully understand the physics of colloidal thruster propulsion technology. Colloidal thruster technology is based on the electrostatic acceleration of small droplets and/or ions that are generated by feeding a conducting fluid through a small capillary and applying a large acceleration potential between the capillary and an extraction electrode. Maximum thrust is obtained when the device is operated in the droplet mode. However, by transitioning to an ion mode, the specific impulse can be greatly increased. Here, we use molecular modeling to study the dynamics of small droplets of ionic liquids (EMIM-BF4) in the presence of large external electric fields. Interatomic and molecular forces are described using a molecular mechanics force field, and the whole ion structure is included. Before an electric field is applied, minimization methods are used to determine the equilibrium structure of the droplet. An electric field is then applied and the resulting motions of droplets and individual ions are observed. In addition, the surface tension of the droplets is calculated from the dynamic simulations. Surface tensions calculated from the simulations agree with macroscopic experimental values within uncertainty. Thus, the results indicate that the Taylor expression for the critical electric field for droplet ionization is order-of-magnitude-correct.

Introduction

THE work reported here is motivated by a desire to fully understand the physics of colloidal thruster propulsion technology [1] when operating in a mode in which direct ion emission from droplets takes place. Our objective is to develop a method to directly model droplet dynamics under exposure to high electric fields and to predict how droplets ionize and the resulting ion and ion cluster distributions and trajectories. We use molecular modeling to study the dynamics of small droplets of ionic liquids. Before an electric field is applied, minimization methods are used to determine the equilibrium structure of the droplet. An electric field is then applied and the resulting motions of droplets and individual ions are observed. We also carry out simulations to explore the surface tension of small droplets, because theoretical expressions for droplet stability are based on a balance between electrostatic and surface tension forces that may not apply at the nanoscale.

Colloidal thruster technology is based on the electrostatic acceleration of small droplets that are generated by feeding a conducting fluid through a small capillary and applying a large acceleration potential [2]. A typical layout is shown in Fig. 1. Experiments have shown that best results are achieved when the system is operated in the cone mode, which is achieved when the volumetric flow rate lies between the limits (Fernandez de la Mora and Loscertales [3])

$$\frac{\gamma\varepsilon_0\varepsilon}{\rho K} < Q < (\sim 20 \text{ to } 30)\cdot\frac{\gamma\varepsilon_0\varepsilon}{\rho K} \tag{1}$$

where g is the liquid surface tension, e_0 is the permittivity of free space, e is the dielectric constant of the fluid, r is the density, and K is the electrical conductivity. In this limit of very low flow rate, the electrostatic field causes a very narrow jet of charged liquid to form at the tip of the cone. The jet then breaks down into fairly monodisperse and small droplets via the classical Rayleigh mechanism. Scaling arguments (Fernandez de la Mora and Loscertales [3], Rosell-Llompart and Fernandez de la Mora [4], Ganan-Calvo [5], and Chen and Pui [6]) show that the droplet diameters are about

$$D_d = g(\varepsilon)\left(\frac{Q\varepsilon\varepsilon_0}{K}\right)^{1/3} = g(\varepsilon)r^* \tag{2}$$

where $g(\varepsilon)$ is an empirical factor of order unity, and r^* is a characteristic length scale for the radius of the jet near its base

$$r^* \equiv \left(\frac{\varepsilon\varepsilon_0 Q}{K}\right)^{1/3} \tag{3}$$

For electrical conductivities typical of propellants that would be useful for colloid propulsion, droplets are generated with diameters of a few tens of nanometers.

The droplets are subsequently accelerated to high velocities after leaving the nozzle; specific impulses I_{sp} of a few thousand seconds have been demonstrated (although at reasonable applied voltages, they are limited to several hundred seconds.) The specific impulse and thrust of a colloidal thruster is given by

$$I_{sp} = \frac{1}{g}\sqrt{2\frac{q}{m}V_a} \quad \text{and} \quad T = mu_e = gmI_{sp} \tag{4}$$

where q/m is the charge-to-mass ratio of the droplets, and V_a the acceleration voltage. Using the preceding scaling arguments, these can be rewritten as (Gamero-Castano and Hruby [7]):

$$I_{sp} \sim \frac{1}{g}\left(\frac{2V_a f(\varepsilon)}{\rho}\right)^{1/2}\left(\frac{K\gamma}{Q\varepsilon}\right)^{1/4} \text{ and } T \sim (2V_a\rho f(\varepsilon))^{1/2}\left(\frac{K\gamma Q^3}{\varepsilon}\right)^{1/4} \tag{5}$$

For a given propellant, increasing the flow rate increases thrust but reduces specific impulse. If Q in these relations is written $Q = \phi Q_{\min}$, then it is seen that

$$I_{sp} \sim K^{1/2} \quad \text{and} \quad T \sim K^{-1/2} \tag{6}$$

Thus, if high specific impulse is desired, it is important to work with propellants that have large electrical conductivity. Ionic liquids are attractive propellants for colloid propulsion due to large electrical conductivity and low vapor pressure. This special class of compounds (Welton [8], McEwen et al. [9], and Widegren et al. [10])

Received 7 November 2006; revision received 25 January 2008; accepted for publication 18 June 2008.

*Professor, Center for Combustion and Environmental Research, Department of Mechanical Engineering, 427 UCB. Associate Fellow AIAA.

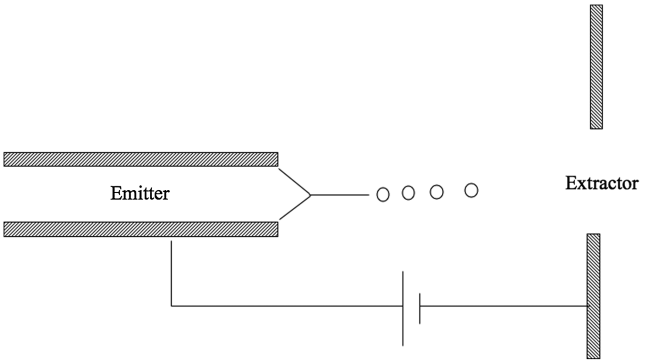

Fig. 1 Typical electrospray configuration.

has opened up the ability to select propellants optimized for specific mission needs.

In addition to the droplet mode of operation, it has been demonstrated that with suitable propellant and operating conditions, the direct emission of ions from the cone tip and from drops can contribute substantially to the specific impulse (Gamero-Castano and Fernandez de la Mora [11] and Romero-Sanz et al. [12].) At smaller values of K/Q, ions do not significantly contribute to the total current flow. However, as K/Q is increased and the droplet diameters decrease, ions begin to evaporate from the drops. Early workers noted that at a critical value of an imposed electric field, a charged droplet would begin to jet and otherwise disintegrate. By carrying out a simple force balance, Taylor showed [13] that the critical value of the electric field is about (value calculated for $r = 55$ Å and surface tension of 58 dyne/cm)

$$E_c \cong \frac{1.625}{\sqrt{8\pi}}\sqrt{\frac{2\gamma}{\varepsilon_0 r}} \approx 0.5 \times 10^9 \ \frac{\text{V}}{\text{m}} \tag{7}$$

In recent work, Chiu et al. [14] used molecular beam/mass spectrometry to analyze the plume of an electrospray with 1-ethyl-3-methylimidazolium bis(trifluoromethylsulfonyl)imide (EMI-Im)[†] as the propellant. They showed that for the operating conditions imposed, at least two positive ion cluster sizes and a background that is likely fragmented droplets are observed. It is this behavior that we wish to explore because it is important in understanding how the plume is formed and the effect of cluster size distribution on thrust.

In the following, we present the theoretical methods used in the study. We then outline how we assemble charged droplets and determined their likely equilibrium configurations. We then present the results of simulations for some different-sized droplets exposed to external electric fields. Next, we present molecular dynamics simulations intended to determine the surface tension of small droplets. This is followed by a discussion of the findings, a summary, and conclusions.

Theoretical Methods

The molecular dynamics simulations were carried out using a modified version of the Tinker [15] program set and an empirical force field developed by de Andrade et al. [16] based on the AMBER [17] force field. Molecular dynamics involves solving Newton's law for each atom in the system. The force acting on an atom is equal to the negative of the gradient of the potential energy plus the electrostatic force imposed by any external field. Thus,

$$\mathbf{a} = \frac{\mathbf{F}}{m} + q\mathbf{E} \tag{8}$$

where we have modified the Tinker code to include the electrostatic force term in all the available solvers.

In the AMBER methodology, the potential energy function is of the form

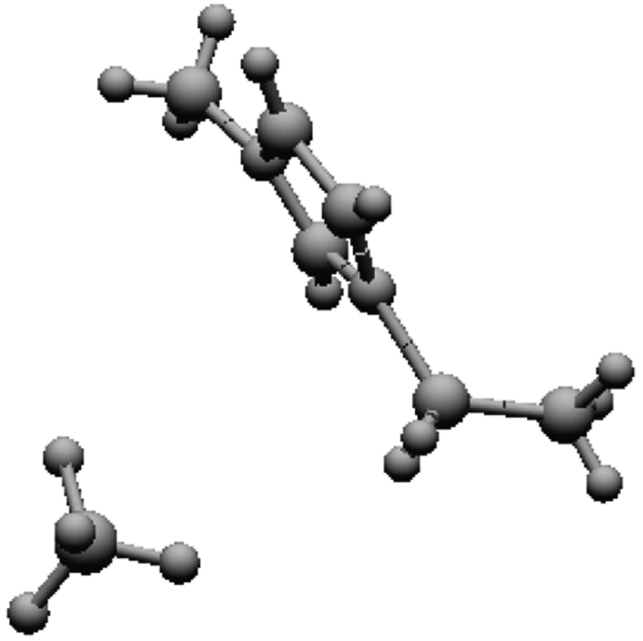

Fig. 2 Optimized EMIM/BF_4 pair.

$$V = \sum_{\text{bonds}} K_r(r - r_{\text{eq}})^2 + \sum_{\text{angles}} K_\theta(\theta - \theta_{\text{eq}})^2 + \sum_{\text{dihedrals}} V_n(1 + \cos(n\phi - \gamma)) + \sum_{i=1}^{N-1}\sum_{j>i}^{N}\left[\frac{A_{ij}}{R_{ij}^{12}} - \frac{B_{ij}}{R_{ij}^{6}} + \frac{q_i q_j}{r_{ij}}\right] \tag{9}$$

The first term is harmonic bond stretching, the second term is three-atom bond bending, and the third term is four-atom torsion. The final term includes nonbonded Lennard-Jones attraction and repulsion and electrostatic interaction. A_{ij} and B_{ij} are written in terms of the well-depth and size parameters ε and σ:

$$A_{ij} = 4\varepsilon_{ij}\sigma_{ij}^{12} \qquad B_{ij} = 4\varepsilon_{ij}\sigma_{ij}^{6} \tag{10}$$

The Lennard-Jones parameters are obtained from the Lorentz–Berthelot mixing rule:

$$\varepsilon_{ij} = \sqrt{\varepsilon_i \varepsilon_j} \qquad \sigma_{ij} = (\sigma_{ii} + \sigma_{jj})/2 \tag{11}$$

De Andrade et al. [16] carried out quantum mechanical calculations to obtain the electron density distribution and then assigned charge to each atom in EMIM and BF_4 using the restrained electrostatic potential (RESP) [18] fitting approach.

Building Drops

We carried out the study by building individual droplets of the ionic liquid 1-ethyl-3-methyl imidazolium tetraflouroborate (EMIM-BF_4[‡]). We first optimized the structure of individual ions and ion pairs. With these structures, we started to build individual drops by randomly placing ions with a spherical volume. However, none of these structures proved to be stable. Upon running molecular dynamics simulations in a zero electric field, these randomly oriented structures immediately vaporized. Further study revealed that stability at room temperature and the corresponding low vapor pressure of ionic liquids arises from the fact that ordered structures are formed in the solid state that persist following melting (Wilkes and Zaworotko [19], Dieter et al. [20], and Del Popolo and Voth [21]). We then optimized the geometry of the EMIM/BF_4 pair, as shown in Fig. 2. Using this base structure, we created cubic droplets

[†]Data available online at http://www.sigmaaldrich.com.

[‡]Data available online at http://www.sigmaaldrich.com.

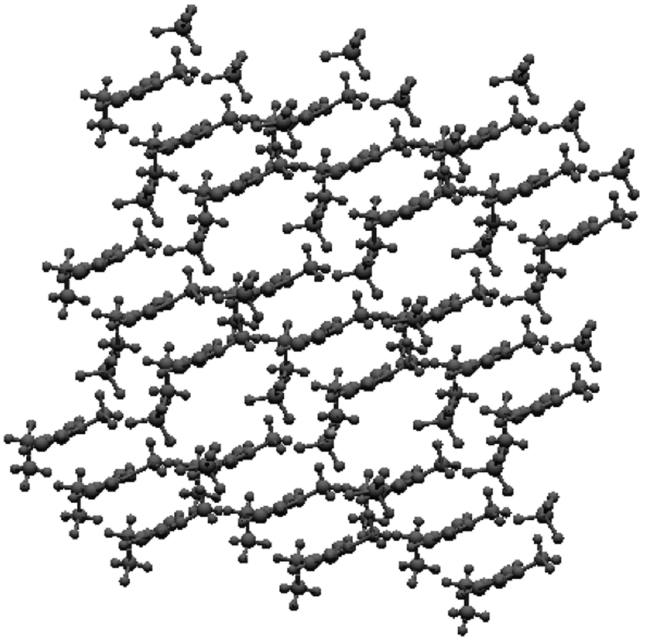

Fig. 3 Initial drop structure.

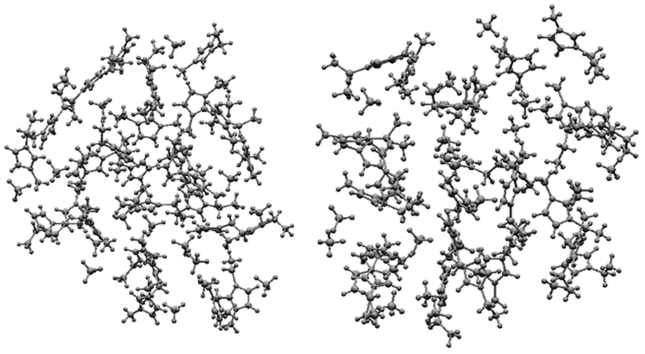

a) b)

Fig. 4 Structure a) minimized and b) following a 100-ps molecular dynamics run.

with ordered structure. An example of an initial droplet structure with 27 EMIM ions and 26 BF_4 ions is shown in Fig. 3.

We took two approaches to determine the equilibrium structure of droplets. First, we used a limited-memory L-BFGS (Broyden–Fletcher–Goldfarb–Shanno) minimization of an input structure over Cartesian coordinates. This resulted in droplets that were approximately spherical, although the larger the droplets, the less spherical they were. We also ran molecular dynamic simulations and observed that the droplets, which started out as highly ordered cubes, randomized to some degree and approached a spherical shape. Figure 4a is the initial geometry shown in Fig. 3 following energy minimization. Figure 4b shows the state of the same initial structure after a 100-ps molecular dynamics run. In both cases, the initial temperature was set to 300 K. For droplets of the size shown here, there is a substantial amount of thermal motion with respect to the drop dimensions. Thus, the drop undergoes obvious shape changes on the thermal motion time scale.

Droplet Ionization

Using the results of either the minimization procedure or molecular dynamics calculation, we then imposed an external electric field of varying strength to the droplets and observed their behavior. All the simulations were for initially randomized energies based on a temperature of 300 K and were run in vacuum. We carried out 100-ps calculations for drops with 8/7, 27/26, and 125/124 EMIM/BF_4 ratios. Thus, each drop had a net positive charge of

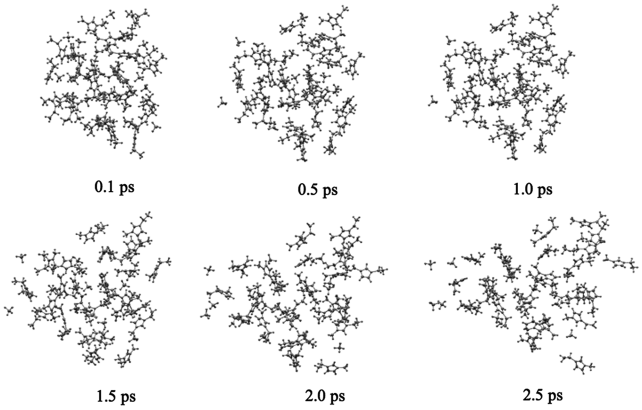

Fig. 5 Sequence of frames from a simulation of a droplet initially with 27 EMIM positive ions and 26 BF_4 negative ions.

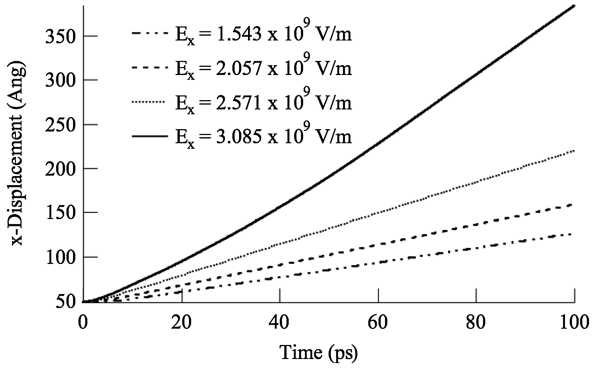

Fig. 6 *X* displacement of the drop center of mass (27/26 droplet.)

unity. These three drops had initial diameters of approximately 21, 38, and 50 Å, respectively. In each case, we applied an electric field in the x direction with a value $E_x = 0.5142 \times 10^9$, 1.028×10^9, 1.543×10^9, 2.057×10^9, or 3.085×10^9 V/m.

In all cases, the drops were stable for the entire 100 ps at $E_x = 0.5142 \times 10^9$ V/m. They retained their starting configuration except for thermal motion, but accelerated in the direction of the applied field according to their net charge. As the field was increased, individual ions began to be stripped off the drops. However, the stripping process was very uneven, and there was a wide distribution of cluster sizes ranging from single ions to, at the lower field intensities, a remaining droplet that retained most of the initial mass. Finally, at the highest field applied, the drops were stripped of ions within a few hundred femptoseconds. Figure 5 shows a series of images from the simulation of a 27/26 droplet with $E_x = 2.057 \times 10^9$ V/m.

To quantify the results somewhat, we calculated several quantities as a function of time. The first were center-of-mass coordinates for all the starting mass. The results for a particular set of runs of a 27/26 drop are shown in Fig. 6. As can be seen, the center of mass drifts in the positive x direction throughout the 100-ps simulation and the drift increases with increasing field strength.

We next calculated the outermost range of motion of ions in the three coordinate directions. The x-coordinate results are shown in Fig. 7 for the 27/26 drop. The displacement-time curves are somewhat odd in that there is more total drift in the $\pm x$ direction for the lower values of the applied electric field. This appears to be caused by space charge effects. At higher field strengths, numerous ions are stripped from the starting droplet. This imparts additional momentum in the $\pm y$ and/or $\pm z$ directions. Figure 8 shows the x-direction spatial distribution of ions at 100 ps for an electric field of 3.085×10^9 V/m. The histogram bins are 200 Å wide. Figures 9 and 10 show the spatial distributions in the y and z directions for the same electric field with 5-Å-wide bins. The amount of spread in the offaxis directions is much smaller, as would be expected.

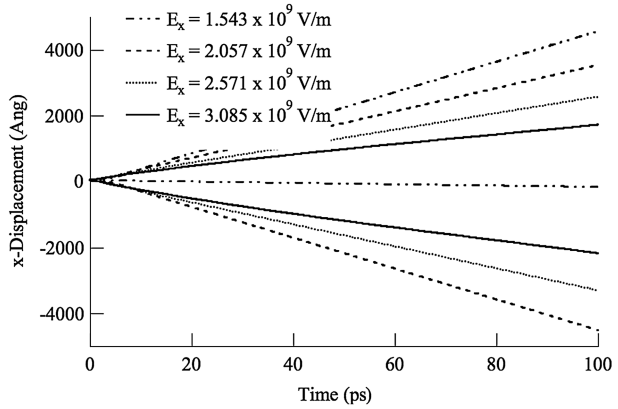

Fig. 7 Displacement-time curves for the outermost atoms in the x coordinate direction (27/26 droplet.)

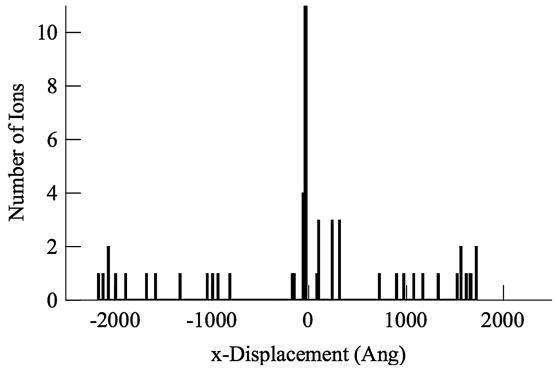

Fig. 8 The x displacement spatial distribution of ions at 100 ps (27/26 droplet with $E_x = 3.085 \times 10^9$ V/m.)

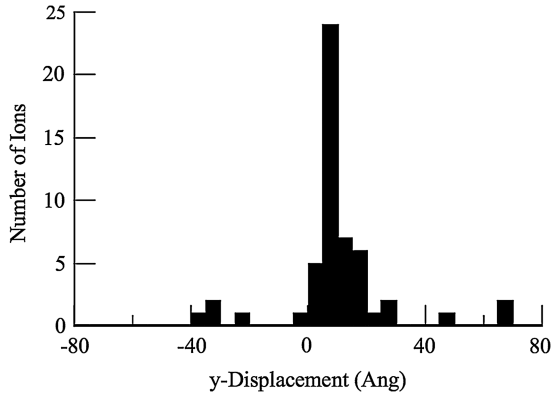

Fig. 9 The y displacement spatial distribution of ions at 100 ps (27/26 droplet with $E_x = 3.085 \times 10^9$ V/m.)

To explore the results in more detail, we stored the total and applied electrostatic forces on each ion during the simulations. The applied electrostatic force should remain constant, but Lennard-Jones and interatomic Coulomb forces will vary, depending on the relative positions of the ions. Indeed, the early effect of space charge and thermal state on the dynamic initial plume formation results in the observed long-time behavior.

To illustrate the effect of the initial thermal state, we compared the results for several runs in which the electric field was held constant and the random generator seed changed between runs. This has the effect of generating a different random initial thermal state. The initial drop position and geometry was held constant. The results are shown in Fig. 11 for six simulations of an 8/7 droplet. Even within the first 10 ps, there is over a 100-Å spread in the maximum displacement of outermost ions due to variation in thermal initial conditions.

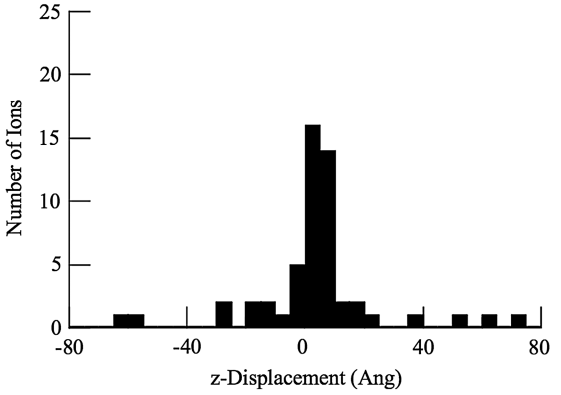

Fig. 10 The z displacement spatial distribution of ions at 100 ps (27/26 droplet with $E_x = 3.085 \times 10^9$ V/m.)

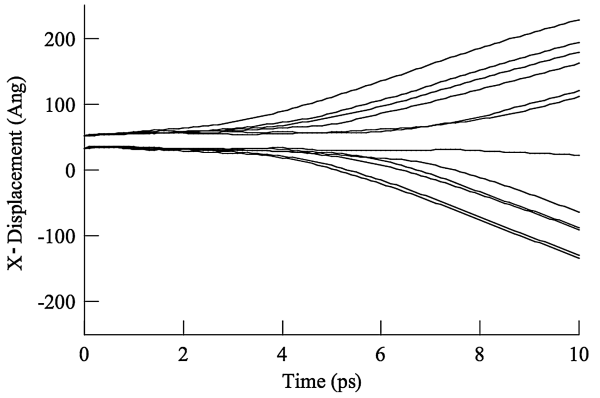

Fig. 11 Displacement-time curves for the outermost atoms in the x coordinate direction for six runs of an 8/7 drop with random initial thermal velocity distributions.

Surface Tension

To apply the Taylor expression for a critical electric field requires the surface tension. Although macroscopic measurements are available, there is a question about how the surface tension behaves for such small droplets. To assess this issue for practical drop diameters, we have estimated surface tension using molecular dynamics methods. For drops, the condition for mechanical equilibrium leads to the Laplace equation

$$\Delta P = \frac{2\gamma_s}{R_s} \tag{12}$$

where γ_s is the surface tension referenced to a surface of tension R_s and ΔP is the pressure difference between the interior of the drop and the exterior (the latter being essentially zero in our case.) For small drops, there can be considerable temporal variability in local properties, including both pressure and radius. Thus, the details of how they are obtained from the simulations are important. We have followed Thompson et al. [22] to calculate the pressure normal to spherical surfaces about the drop center of mass as a function of radius by adding kinetic and configurational terms:

$$P(r) = kT\rho(r) + p_U(r) \tag{13}$$

where

$$p_U(r) = \frac{1}{4\pi r^2}\sum_k f_k \tag{14}$$

Here, the k in Eq. (13) is Boltzmann's constant, T is the temperature, n is the number density, and p_U is the configuration contribution to the normal pressure. The sum in the expression for p_U is overall

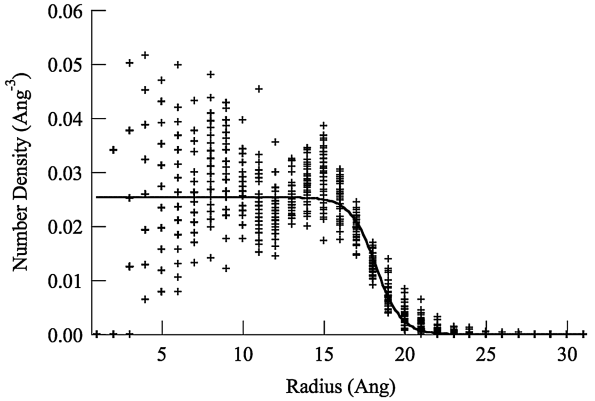

Fig. 12 Number density profile in a 27/26 drop.

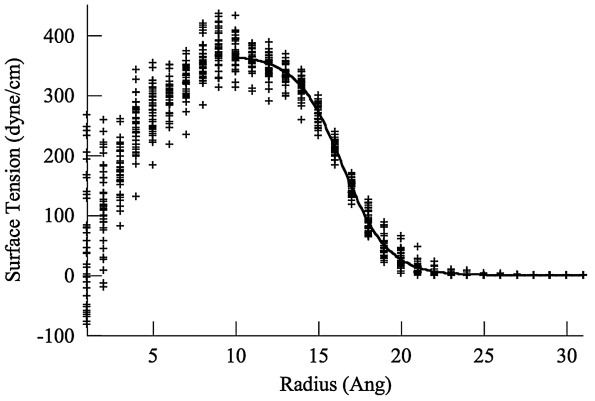

Fig. 13 Surface tension profile in a 27/26 drop.

pairwise normal forces f_k across a sphere of radius r referenced to the center of mass.

The density as a function of radius is calculated by counting the number of atoms in a small spherical shell about each value of the radius following Nijmeijer et al. [23]. The density data are then fit with a tanh regression curve that is used to locate the 50% radius of the drop. This radius is used as the surface of tension and to select the value of the pressure to use in the Laplace equation in recovering the surface tension. An example of the density for 27/26 drops is shown in Fig. 12. For numerical calculations, 1000 separate realizations of a dynamic simulation are averaged, although we have only plotted 36 to illustrate our results.

The surface tension distribution for a 27/26 drop is shown in Fig. 13. (Again, only 36 realizations have been plotted to illustrate our results.) For this particular case, the average surface tension is 88.09 dyne/cm. However, the uncertainty is very large, perhaps as high as ±50%. (The actual uncertainty is difficult to calculate. Although the parameters of the fit are quite certain due to the large number of realizations, a glance at Fig. 12 will reveal that defining the actual surface of tension is somewhat arbitrary.) Thus, within uncertainty, the simulation results are the same as reported experimental values [24]. Hence, Taylor's expression for the critical electric field is a reasonable way to obtain an order-of-magnitude estimate for the onset of direct ionization from droplets of ionic liquids.

Conclusions

Calculations indicate that the surface tension is not a strong function of droplet radius. Thus, the Taylor expression using macroscopic surface tensions for the critical electric field strength is approximately correct, but only in the order-of-magnitude sense. The transition to ion emission takes place continuously as the field strength is increased, starting with the stripping of one or a few ions and finally reaching a point at which the droplet is ripped apart in less than a picosecond. The process is affected by thermal motion, most especially at lower field strengths. The energy required to remove a single ion from a drop is determined by the sum of the forces acting on the ion plus or minus the instantaneous thermal translational energy of the ion. In this case, the ion–ion forces are caused by Lennard-Jones and electrostatic interactions. Thus, which particular ion is initially stripped depends on location and translational energy. However, at the larger field strengths, the applied electrostatic force is sufficient to overcome attractive forces and the drop proceeds to disintegrate. The long-time ion plume behavior is strongly influenced by the initial thermal motion and space charge effects. The ionization process does not necessary produce single ions. At lower field strengths, a range of cluster sizes can be produced. This is observed in the molecular-beam/mass-spectrometry measurements of Chiu et al. [14], as described in the Introduction.

Acknowledgments

Support for this work was provided as part of a Small Business Technology Transfer project funded by the U.S. Air Force Office of Scientific Research through TDA Reseach, Inc. The Technical Contract Monitor was Mitat Birkan. James Nabity of TDA Research was the Principle Investigator on the STTR, and John W. Daily the Principle Investigator for the work carried out at the University of Colorado. The author gratefully acknowledges fruitful conversations with James Nabity, David Kassoy, Michael Micci, and Juan Fernandez De La Mora.

References

[1] Mueller, J., "Thruster Options for Microspacecraft: A Review and Evaluation of Existing Hardware and Emerging Technologies," AIAA Paper 97-3053, 1997.

[2] Khayms, V., "Advanced Propulsion for Microsatellites," Ph.D. Thesis, Department of Aeronautics and Astronautics, Massachusetts Inst. of Technology, Cambridge, MA, 2000.

[3] Fernandez de La Mora, J., and Loscertales, I. G., "The Current Emitted by Highly Conducting Taylor Cones," *Journal of Fluid Mechanics*, Vol. 260, 1994, pp. 155–184. doi:10.1017/S0022112094003472

[4] Rosell-Llompart, J., and Fernandez de la Mora, J., "Generation of Monodisperse Droplets 0.3 to 4 mm in Diameter from Electrified Cone Jets of Highly Conducting and Viscous Liquids," *Journal of Aerosol Science*, Vol. 25, No. 6, 1994, pp. 1093–1119. doi:10.1016/0021-8502(94)90204-6

[5] Ganan-Calvo, A. M., "Cone-Jet Analytical Extension of Taylor's Electrostatic Solution and the Asymptotic Universal Scaling Laws in Electrospraying," *Physical Review Letters*, Vol. 79, No. 2, 1997, pp. 217–220. doi:10.1103/PhysRevLett.79.217

[6] Chen, D.-R., and Pui, D. Y. H., "Experimental Investigation of Scaling Laws For Electrospraying: Dielectric Constant Effect," *Aerosol Science and Technology*, Vol. 27, No. 3, 1997, pp. 367–380. doi:10.1080/02786829708965479

[7] Gamero-Castano, M., and Hruby, V., "Electrospray as a Source of Nanoparticles for Efficient Colloid Thrusters," AIAA Paper AIAA 2000-3265, 2000.

[8] Welton, T., "Room-Temperature Ionic Liquids: Solvents for Synthesis and Catalysis," *Chemical Reviews (Washington, DC)*, Vol. 99, No. 8, 1999, pp. 2071–2083. doi:10.1021/cr980032t

[9] McEwen, A. B., Ngo, H. L., LeCompte, K., and Goldman, J. L., "Electrochemical Properties of Imidazolium Salt Electrolytes for Electrochemical Capacitor Applications," *Journal of the Electrochemical Society*, Vol. 146, No. 5, 1999, pp. 1687–1695. doi:10.1149/1.1391827

[10] Widegren, J. A., Laesecke, A., and Magee, J. W., "The Effect of Dissolved Water on the Viscosities of Hydrophobic Room-Temperature Ionic Liquids," *Chemical Communications (Cambridge)*, No. 12, 2005, pp. 1610–1612. doi:10.1039/b417348a

[11] Gamero-Castano, M., and Fernandez de la Mora, J., "Direct Measurement of Ion Evaporation Kinetics from Electrified Liquid Surfaces," *Journal of Chemical Physics*, Vol. 113, No. 2, 2000, pp. 815–832. doi:10.1063/1.481857

[12] Romero-Sanz, I., Bocanegra, R., and Fernandez de la Mora, J., "Source of Heavy Molecular Ions Based on Taylor Cones of Ionic Liquids Operating in the Pure Ion Evaporation Regime," *Journal of Applied Physics*, Vol. 94, No. 5, 2003, pp. 3599–3605. doi:10.1063/1.1598281

[13] Taylor, G. I., "Disintegration of Water Drops in an Electric Field," *Proceedings of the Royal Society of London, Series A: Mathematical and Physical Sciences*, Vol. 280, No. 1382, 1964, pp. 383–387. doi:10.1098/rspa.1964.0151

[14] Chiu, Y.-H., Gaeta, G., Heine, T. R., Dressler, R. A., and Levandier, D. J., "Analysis of the Electrospray Plume from the EMI-Im Propellant Externally Wetted on a Tungsten Needle," 42nd AIAA/ASME/SAE/ASEE Joint Propulsion Conference and Exhibit, Sacramento, CA, AIAA Paper 2006-5010, 9–12 July 2006.

[15] TINKER, Software Package, Ver. 4.2, Washington Univ. in St. Louis, St. Louis, MO; available online at http://dasher.wustl.edu/tinker.

[16] de Andrade, J., Boes, E. S., and Stassen, H., "Computational Study of Room Temperature Molten Salts Composed by 1-Alkyl-3-Methyl-imidazolium Cations: Force-Field Proposal and Validation," *Journal of Chemical Physics*, Vol. 106, No. 51, 2002, pp. 13344–13351.

[17] Cornell, W. D., Cieplak, P., Bayly, C. I., Gould, I. R., Merz, K. M., Jr., Ferguson, D. M., Spellmeyer, D. C., Fox, T., Caldwell, J. W., and Kollman, P. A., "A Second Generation Force Field for the Simulation of Proteins, Nucleic Acids, and Organic Molecules," *Journal of the American Chemical Society*, Vol. 117, No. 19, 1995, pp. 5179–5197. doi:10.1021/ja00124a002

[18] Bayly, C. I., Cieplak, P., Cornell, W. D., and Kollman, P. A., "A Well-Behaved Electrostatic Potential Based Method Using Charge Restraints for Deriving Atomic Charges: The RESP Model," *Journal of Physical Chemistry*, Vol. 97, No. 40, 1993, pp. 10269–10280. doi:10.1021/j100142a004

[19] Wilkes, J. S., and Zaworotko, M. J., "Air and Water Stable 1-Ethyl-3-Methylimidazolium Based Ionic Liquids," *Journal of the Chemical Society, Chemical Communications*, 1992, No. 13, pp. 965–967. doi:10.1039/c39920000965

[20] Dieter, K. M., Dymek, C. J., Jr., Heimer, N. E., Rovang, J. W., and Wilkes, J. S., "Ionic Structure and Interactions in 1-Methyl-3-Ethylimidazolium Chloride-A1C13 Molten Salts," *Journal of the American Chemical Society*, Vol. 110, No. 9, 1988, pp. 2722–2726. doi:10.1021/ja00217a004

[21] Del Popolo, M. G., and Voth, G. A., "On the Structure and Dynamics of Ionic Liquids," *Journal of Physical Chemistry B*, Vol. 108, No. 5, 2004, pp. 1744–1752. doi:10.1021/jp0364699

[22] Thompson, S. M., Gubbins, K. E., Walton, J. P. R. B., Chantry, R. A. R., and Rowlinson, J. S., "A Molecular Dynamics Study of Liquid Drops," *Journal of Chemical Physics*, Vol. 81, No. 1, 1984, pp. 530–542. doi:10.1063/1.447358

[23] Nijmeijer, M. J. P., Bruin, C., van Woerkom, A. B., and Bakker, A. F., "Molecular Dynamics of the Surface Tension of a Drop," *Journal of Chemical Physics*, Vol. 96, No. 1, 1992, pp. 565–576. doi:10.1063/1.462495

[24] Krupenkin, T. N., Taylor, J. A., Schneider, T. M., and Yang, S., "From Rolling Ball to Complete Wetting: The Dynamic Turning of Liquids on Nanostructured Surfaces," *Langmuir*, Vol. 20, No. 10, 2004, pp. 3824–3827. doi:10.1021/la036093q

E. Choueiri
Associate Editor